Filomat 37:19 (2023), 6365–6372
https://doi.org/10.2298/FIL2319365L

Published by Faculty of Sciences and Mathematics,
University of Niš, Serbia
Available at: http://www.pmf.ni.ac.rs/filomat

A decoupled algorithm for fluid-fluid interaction at small viscosity

Wei Li[a], Pengzhan Huang[a,*]

[a]*College of Mathematics and System Sciences, Xinjiang University, Urumqi, 830017, P.R. China*

Abstract. In this paper, a decoupled finite element algorithm is proposed for solving the fluid-fluid interaction at small viscosity. The basic idea of the presented algorithm is to first solve an artificial viscosity elliptic problem with explicit treatment for nonlinear interface conditions, and then solve an artificial viscosity Stokes problem to correct the previous solution. The unconditional stability is established and the efficiency is illustrated by some numerical tests.

1. Introduction

The paper aims to design the decoupled finite element algorithm for the nonlinear fluid-fluid interaction model in the case of small viscosities. The model is given as follows [6, 15]. Find the fluid velocities $\mathbf{u}_i : (0,T]\times\Omega_i \to \mathbb{R}^d$ and pressures $p_i : (0,T]\times\Omega_i \to \mathbb{R}$ satisfying

$$\begin{aligned} \mathbf{u}_{i,t} - \nu_i\Delta\mathbf{u}_i &= \mathbf{f}_i - \mathbf{u}_i\cdot\nabla\mathbf{u}_i - \nabla p_i, && \text{in } \Omega_i,\\ -\nu_i\mathbf{n}_i\cdot\nabla\mathbf{u}_i\cdot\tau &= \kappa|\mathbf{u}_i-\mathbf{u}_j|(\mathbf{u}_i-\mathbf{u}_j)\cdot\tau, \quad \mathbf{u}_i\cdot\mathbf{n}_i = 0, && \text{on } I, \text{ for } i,j=1,2 \text{ and } i\neq j,\\ \nabla\cdot\mathbf{u}_i = 0, \quad \mathbf{u}_i(0,\mathbf{x}) &= \mathbf{u}_{i,0}(\mathbf{x}), && \text{in } \Omega_i,\\ \mathbf{u}_i &= 0, && \text{on } \Gamma_i := \partial\Omega_i\backslash I, \end{aligned} \tag{1}$$

where $\Omega\subset\mathbb{R}^d$ $(d=2,3)$ is a bounded domain and consists of two sub-domains Ω_1 and Ω_2 coupled across their shared interface I. For $i=1,2$, $\nu_i>0$ present the kinematic viscosities, $\mathbf{f}_i$ are the body forces, and $\kappa>0$ is the friction coefficient. Besides, $|\cdot|$ represents the Euclidean norm, the vectors $\mathbf{n}_i$ are the unit normals on $\partial\Omega_i$, and $\boldsymbol{\tau}$ is any vector on I such that $\boldsymbol{\tau}\cdot\mathbf{n}_i = 0$.

Due to the practical importance of the coupled model (1), many research works have been devoted recently to considering various decoupled numerical methods. Recently, Connors et al. [6] have presented a decoupled time stepping method called the geometric averaging method, which is unconditionally stable and two-step (or three-level) scheme. Based on the unconditional stability of the geometric averaging method, several stable schemes have undergone some evolution and been well further developed [2, 5, 9–11, 13, 14, 16]. In particular, based on the geometric averaging method, the variational multiscale stabilization is applied to solve the fluid-fluid interaction problem at high Reynolds numbers [3]. Moreover, Aggul

2020 *Mathematics Subject Classification*. Primary 65M60; Secondary 65M32.
Keywords. Fluid-fluid interaction model; Finite element method; Unconditional stability; Small viscosity.
Received: 27 September 2022; Accepted: 04 March 2023
Communicated by Marko Nedeljkov
Research supported by Postgraduate Research and Innovation Program of Xinjiang Uygur Autonomous Region (grant number XJ2022G019) and Xinjiang Key Laboratory of Applied Mathematics (grant number XJDX1401)
* Corresponding author: Pengzhan Huang
Email addresses: lywinxjst@yeah.net (Wei Li), hpzh@xju.edu.cn (Pengzhan Huang)

and Kaya [4] have combined the defect-deferred correction method with the subgrid artificial viscosity. A penalty projection method is employed for the fluid-fluid interaction problem, where the grad-div stabilization term is added to impose the mass conservation [1]. Further, an unconditionally energy stable finite element scheme is designed for the nonlinear fluid-fluid interaction model [12].

In this paper, by combining the idea of scalar auxiliary variable approach by Shen and Xu [17] with the viscosity splitting technique [19], we propose a decoupled finite element algorithm for the fluid-fluid interaction at small viscosity. In this algorithm, we first solve an artificial viscosity elliptic problem with explicit treatment for nonlinear interface conditions, and then solve an artificial viscosity Stokes problem to correct the previous solution. This algorithm is a decoupled, explicit and unconditionally stable one-step scheme. It can deal with the considered problem as the small viscosity well.

2. Preliminaries

We introduce the usual $L^2(\Omega_i)$ norm and its inner product by $\|\cdot\|_0$ and $(\cdot,\cdot)_{\Omega_i}$, respectively. For the mathematical setting of the fluid-fluid interaction model (1), we introduce the following function spaces:

$$\mathbf{X}_i = \{\mathbf{v}_i \in H^1(\Omega_i)^2; \mathbf{v}_i|_{\Gamma_i} = 0; \mathbf{v}_i \cdot \mathbf{n}_i = 0 \text{ on } I\}, \quad M_i = \{q_i \in L^2(\Omega_i); (q_i, 1) = 0\}.$$

For $\mathbf{f}_i$ an element in the dual space of $\mathbf{X}_i$, its norm is defined by $\|\mathbf{f}_i\|_{-1} = \sup_{\mathbf{v}_i \in \mathbf{X}_i} \frac{|(\mathbf{f}_i, \mathbf{v}_i)|}{\|\nabla \mathbf{v}_i\|_0}$. In particular, all of the above notations are adaptable to the sub-domain Ω_j.

Next, we introduce a scalar auxiliary variable $Q(t) = 1$, which satisfies

$$\frac{\mathrm{d}Q}{\mathrm{d}t} = \sum_{i=1}^{2} \int_I \kappa |\mathbf{u}_i - \mathbf{u}_j|(\mathbf{u}_i - \mathbf{u}_j) \cdot \mathbf{u}_i \mathrm{ds} + Q \sum_{i=1}^{2} \int_I \kappa |\mathbf{u}_i - \mathbf{u}_j|(\mathbf{u}_j - \mathbf{u}_i) \cdot \mathbf{u}_i \mathrm{ds}. \tag{2}$$

Note that the sum of the interaction terms in (2) is zero due to

$$\int_I |\mathbf{u}_i - \mathbf{u}_j|(\mathbf{u}_i - \mathbf{u}_j) \cdot \mathbf{u}_i + |\mathbf{u}_i - \mathbf{u}_j|(\mathbf{u}_j - \mathbf{u}_i) \cdot \mathbf{u}_i \mathrm{ds} = 0.$$

Since $Q(t) = 1$ for the continues case, the interface condition in (1) can be rewritten as

$$-\nu_i \mathbf{n}_i \cdot \nabla \mathbf{u}_i \cdot \boldsymbol{\tau} = Q\kappa |\mathbf{u}_i - \mathbf{u}_j|(\mathbf{u}_i - \mathbf{u}_j) \cdot \boldsymbol{\tau} \quad \text{on } I, \text{ for } i, j = 1, 2, \text{ and } i \neq j. \tag{3}$$

In fact, the scalar auxiliary variable is a scalar function of t which keeps the original continues system. Moreover, the introduction of the scalar auxiliary variable allows us to decouple the nonlinear interaction terms by using a fully explicit scheme, which will be showed in next section. Meanwhile, compared to the implicit/explicit approach, which has the constraint on spatial and temporal steps [18], the presented algorithm is unconditionally stable which will be proved.

Based on the above definitions of the function spaces and scalar auxiliary variable, the corresponding variational formulation of the combination of (1) with (3) is given as follows: find $\mathbf{u}_i : (0, T] \to \mathbf{X}_i$ and $p_i : (0, T] \to M_i$ for all $(v_i, q_i) \in \mathbf{X}_i \times M_i$, $i, j = 1, 2$, $i \neq j$ such that

$$(\mathbf{u}_{i,t}, \mathbf{v}_i) + \nu_i(\nabla \mathbf{u}_i, \nabla \mathbf{v}_i) - (\nabla \cdot \mathbf{v}_i, p_i) + (\nabla \cdot \mathbf{u}_i, q_i) + b(\mathbf{u}_i, \mathbf{u}_i, \mathbf{v}_i) + Q \int_I \kappa |\mathbf{u}_i - \mathbf{u}_j|(\mathbf{u}_i - \mathbf{u}_j)\mathbf{v}_i \mathrm{ds} = (\mathbf{f}_i, \mathbf{v}_i).$$

where $b(\cdot,\cdot,\cdot)$ are defined on $\mathbf{X}_i \times \mathbf{X}_i \times \mathbf{X}_i$ by [7, 8]

$$b(\mathbf{u}_i, \mathbf{v}_i, \mathbf{w}_i) = ((\mathbf{u}_i \cdot \nabla)\mathbf{v}_i, \mathbf{w}_i) + \tfrac{1}{2}((\nabla \cdot \mathbf{u}_i)\mathbf{v}_i, \mathbf{w}_i) = \tfrac{1}{2}((\mathbf{u}_i \cdot \nabla)\mathbf{v}_i, \mathbf{w}_i) - \tfrac{1}{2}((\mathbf{u}_i \cdot \nabla)\mathbf{w}_i, \mathbf{v}_i), \quad \forall \mathbf{u}_i, \mathbf{v}_i, \mathbf{w}_i \in \mathbf{X}_i.$$

3. A decoupled finite element algorithm

From now on, given $N > 0$, let $\{t_n\}_{n=0}^N$ be a uniform partition of $[0, T]$ with time step $\Delta t = \frac{T}{N}$, and $t_n = n\Delta t$. For $i = 1, 2$, let π_i^h be a triangulation of Ω_i and $\pi^h = \pi_1^h \cup \pi_2^h$. The mesh size h is the largest diameter of the element in π^h. Accordingly, assume the finite element spaces $\mathbf{X}_i^h \subset \mathbf{X}_i$ for velocity fields and $M_i^h \subset M_i$ for pressures satisfying discrete Ladyzenskaja-Babuška-Brezzi condition. The MINI finite elements are known to satisfy this condition. Furthermore, $(\mathbf{u}_{i,h}^n, p_{i,h}^n)$ denote the fully discrete approximation to the solution $(\mathbf{u}_i, p_i)$ of (1) at $t = t_n$. Besides, we set $\mathbf{f}_i^n = \mathbf{f}_i(t_n)$.

Then, based on a mixed finite element approximation for spatial discretization, the first order backward Euler scheme for temporal discretization, and explicit treatment for the interface conditions, a fully discrete and decoupled finite element algorithm is proposed, which involves the viscosity splitting technique aiming to deal with the small viscosity.

Step 1: Given $\mathbf{u}_{i,h}^n \in \mathbf{X}_i^h$, $\mathbf{u}_{j,h}^n \in \mathbf{X}_j^h$ and $Q^n \in \mathbb{R}$, for $0 \le n \le N-1$, find $\hat{\mathbf{u}}_{i,h}^{n+1} \in \mathbf{X}_i^h$ and $Q^{n+1} \in \mathbb{R}$ satisfying that for all $\mathbf{v}_{i,h} \in \mathbf{X}_i^h, i, j = 1, 2, i \neq j$,

$$\begin{aligned}&\left(\frac{\hat{\mathbf{u}}_{i,h}^{n+1} - \mathbf{u}_{i,h}^n}{\Delta t}, \mathbf{v}_{i,h}\right) + \nu_i(\nabla\hat{\mathbf{u}}_{i,h}^{n+1}, \nabla\mathbf{v}_{i,h}) + r_i(\nabla\hat{\mathbf{u}}_{i,h}^{n+1} - \nabla\mathbf{u}_{i,h}^n, \nabla\mathbf{v}_{i,h}) + b(\mathbf{u}_{i,h}^n, \hat{\mathbf{u}}_{i,h}^{n+1}, \mathbf{v}_{i,h})\\ &\quad + Q^{n+1}\int_I \kappa|\mathbf{u}_{i,h}^n - \mathbf{u}_{j,h}^n|(\mathbf{u}_{i,h}^n - \mathbf{u}_{j,h}^n)\mathbf{v}_{i,h}\mathrm{d}s = (\mathbf{f}_i^{n+1}, \mathbf{v}_{i,h}),\end{aligned} \tag{4}$$

and

$$\frac{Q^{n+1} - Q^n}{\Delta t} = \sum_{i=1}^2 \int_I \kappa|\mathbf{u}_{i,h}^n - \mathbf{u}_{j,h}^n|(\mathbf{u}_{i,h}^n - \mathbf{u}_{j,h}^n)\hat{\mathbf{u}}_{i,h}^{n+1}\mathrm{d}s + Q^{n+1}\sum_{i=1}^2 \int \kappa|\mathbf{u}_{i,h}^n - \mathbf{u}_{j,h}^n|(\mathbf{u}_{j,h}^n - \mathbf{u}_{i,h}^n)\mathbf{u}_{i,h}^n\mathrm{d}s. \tag{5}$$

where the parameters $r_i \ge 0$ and $Q^0 = 1$.

Step 2: Based on $\hat{\mathbf{u}}_{i,h}^{n+1}$ from (4)-(5), find $(\mathbf{u}_{i,h}^{n+1}, p_{i,h}^{n+1}) \in \mathbf{X}_i^h \times M_i^h$ satisfying that for all $\mathbf{v}_{i,h} \in \mathbf{X}_i^h, q_{i,h} \in M_i^h$,

$$\begin{aligned}&\left(\frac{\mathbf{u}_{i,h}^{n+1} - \hat{\mathbf{u}}_{i,h}^{n+1}}{\Delta t}, \mathbf{v}_{i,h}\right) + \nu_i(\nabla\mathbf{u}_{i,h}^{n+1} - \nabla\hat{\mathbf{u}}_{i,h}^{n+1}, \nabla\mathbf{v}_{i,h}) + r_i(\nabla\mathbf{u}_{i,h}^{n+1} - \nabla\hat{\mathbf{u}}_{i,h}^{n+1}, \nabla\mathbf{v}_{i,h})\\ &\quad - (\nabla\cdot\mathbf{v}_{i,h}, p_{i,h}^{n+1}) + (\nabla\cdot\mathbf{u}_{i,h}^{n+1}, q_{i,h}) = 0.\end{aligned} \tag{6}$$

Remark 3.1. *The above numerical approach uses a fully explicit scheme to decouple the nonlinear interface terms and is unconditionally stable, which will be showed in Theorem 3.3. Additionally, compared with the geometric averaging algorithm (two-step scheme in time) [6], the proposed algorithm is a one-step scheme in time.*

How to solve (4) and (5)?

Firstly, set

$$\hat{\mathbf{u}}_{i,h}^{n+1} = \tilde{\mathbf{u}}_{i,h}^{n+1} + Q^{n+1}\bar{\mathbf{u}}_{i,h}^{n+1}, \quad i = 1, 2. \tag{7}$$

Then, substituting (7) into (4), we have

$$\left(\frac{\tilde{\mathbf{u}}_{i,h}^{n+1} - \mathbf{u}_{i,h}^n}{\Delta t}, \mathbf{v}_{i,h}\right) + \nu_i(\nabla\tilde{\mathbf{u}}_{i,h}^{n+1}, \nabla\mathbf{v}_{i,h}) + b(\mathbf{u}_{i,h}^n, \tilde{\mathbf{u}}_{i,h}^{n+1}, \mathbf{v}_{i,h}) + r_i(\nabla\tilde{\mathbf{u}}_{i,h}^{n+1} - \nabla\mathbf{u}_{i,h}^n, \nabla\mathbf{v}_{i,h}) = (\mathbf{f}_i^{n+1}, \mathbf{v}_{i,h}), \tag{8}$$

and

$$\left(\frac{\bar{\mathbf{u}}_{i,h}^{n+1}}{\Delta t}, \mathbf{v}_{i,h}\right) + \nu_i(\nabla\bar{\mathbf{u}}_{i,h}^{n+1}, \nabla\mathbf{v}_{i,h}) + b(\mathbf{u}_{i,h}^n, \bar{\mathbf{u}}_{i,h}^{n+1}, \mathbf{v}_{i,h}) + r_i\left(\nabla\bar{\mathbf{u}}_{i,h}^{n+1}, \nabla\mathbf{v}_{i,h}\right) + \int_I \kappa|\mathbf{u}_{i,h}^n - \mathbf{u}_{j,h}^n|(\mathbf{u}_{i,h}^n - \mathbf{u}_{j,h}^n)\mathbf{v}_{i,h}\mathrm{d}s = 0. \tag{9}$$

Secondly, substituting (7) into (5), we get

$$\left(\frac{1}{\Delta t}-A^{n+1}\right)Q^{n+1}=\frac{Q^n}{\Delta t}+\sum_{i=1}^{2}\int_I \kappa|\mathbf{u}_{i,h}^n-\mathbf{u}_{j,h}^n|(\mathbf{u}_{i,h}^n-\mathbf{u}_{j,h}^n)\tilde{\mathbf{u}}_{i,h}^{n+1}\mathrm{d}s, \tag{10}$$

where

$$A^{n+1}=\sum_{i=1}^{2}\int_I \kappa|\mathbf{u}_{i,h}^n-\mathbf{u}_{j,h}^n|(\mathbf{u}_{i,h}^n-\mathbf{u}_{j,h}^n)\bar{\mathbf{u}}_{i,h}^{n+1}\mathrm{d}s+\sum_{i=1}^{2}\int_I \kappa|\mathbf{u}_{i,h}^n-\mathbf{u}_{j,h}^n|(\mathbf{u}_{j,h}^n-\mathbf{u}_{i,h}^n)\mathbf{u}_{i,h}^n\mathrm{d}s. \tag{11}$$

Then, according to $\tilde{\mathbf{u}}_{i,h}^{n+1}$ and $\bar{\mathbf{u}}_{i,h}^{n+1}$ obtained from (8) and (9), we get the value of Q^{n+1} by solving (10).

Finally, we obtain $\hat{\mathbf{u}}_{i,h}^{n+1}$ from (7).

Remark 3.2. *The solvability of* (10) *is proven by* $-A^{n+1}>0$. *Setting* $\mathbf{v}_{i,h}=\bar{\mathbf{u}}_{i,h}^{n+1}$ *in* (9) *and summing the ensuing equation from* $i=1,2$ $(i\neq j)$ *get*

$$\frac{1}{\Delta t}\sum_{i=1}^{2}\|\bar{\mathbf{u}}_{i,h}^{n+1}\|_0^2+\sum_{i=1}^{2}\left(\nu_i\|\nabla\bar{\mathbf{u}}_{i,h}^{n+1}\|_0^2+r_i\|\nabla\bar{\mathbf{u}}_{i,h}^{n+1}\|_0^2\right)+\sum_{i=1}^{2}\int_I \kappa|\mathbf{u}_{i,h}^n-\mathbf{u}_{j,h}^n|(\mathbf{u}_{i,h}^n-\mathbf{u}_{j,h}^n)\bar{\mathbf{u}}_{i,h}^{n+1}\mathrm{d}s=0. \tag{12}$$

Adding (11) *and* (12), *we arrive at*

$$\frac{1}{\Delta t}\sum_{i=1}^{2}\|\bar{\mathbf{u}}_{i,h}^{n+1}\|_0^2+\sum_{i=1}^{2}\left(\nu_i\|\nabla\bar{\mathbf{u}}_{i,h}^{n+1}\|_0^2+r_i\|\nabla\bar{\mathbf{u}}_{i,h}^{n+1}\|_0^2\right)+A^{n+1}=\sum_{i=1}^{2}\int_I \kappa|\mathbf{u}_{i,h}^n-\mathbf{u}_{j,h}^n|(\mathbf{u}_{j,h}^n-\mathbf{u}_{i,h}^n)\mathbf{u}_{i,h}^n\mathrm{d}s.$$

We assert $-A^{n+1}>0$.

In the following part of this section, we analyze the stability of (4)-(6).

Theorem 3.3. *Assume initial values* $\mathbf{u}_i^0$ *and body forces* $\mathbf{f}_i$ $(i=1,2)$ *of the algorithm* (4)-(6) *satisfying*

$$\|\mathbf{u}_{1,h}^0\|_0^2+\|\mathbf{u}_{2,h}^0\|_0^2+r_1\Delta t\|\nabla\mathbf{u}_{1,h}^0\|_0^2+r_2\Delta t\|\nabla\mathbf{u}_{2,h}^0\|_0^2+|Q^0|^2+\Delta t\sum_{n=0}^{N-1}\nu_1^{-1}\|\mathbf{f}_1^{n+1}\|_{-1}^2+\Delta t\sum_{n=0}^{N-1}\nu_2^{-1}\|\mathbf{f}_2^{n+1}\|_{-1}^2\leq C,$$

then there holds

$$\begin{aligned}
&\sum_{i=1}^{2}\|\mathbf{u}_{i,h}^N\|_0^2+\sum_{n=0}^{N-1}\sum_{i=1}^{2}\left(\|\mathbf{u}_{i,h}^{n+1}-\hat{\mathbf{u}}_{i,h}^{n+1}\|_0^2+\|\hat{\mathbf{u}}_{i,h}^{n+1}-\mathbf{u}_{i,h}^n\|_0^2\right)+|Q^N|^2+\sum_{n=0}^{N-1}|Q^{n+1}-Q^n|^2\\
&+\sum_{i=1}^{2}r_i\Delta t\|\nabla\mathbf{u}_{i,h}^N\|_0^2+\Delta t\sum_{n=0}^{N-1}\sum_{i=1}^{2}\nu_i\|\nabla\mathbf{u}_{i,h}^{n+1}\|_0^2+\Delta t\sum_{n=0}^{N-1}\sum_{i=1}^{2}\left((r_i+\nu_i)\|\nabla\mathbf{u}_{i,h}^{n+1}-\nabla\hat{\mathbf{u}}_{i,h}^{n+1}\|_0^2+r_i\|\nabla\hat{\mathbf{u}}_{i,h}^{n+1}-\nabla\mathbf{u}_{i,h}^n\|_0^2\right)\\
&+2(Q^{n+1})^2\Delta t\sum_{n=0}^{N-1}\int_I \kappa|\mathbf{u}_{1,h}^n-\mathbf{u}_{2,h}^n|(\mathbf{u}_{1,h}^n-\mathbf{u}_{2,h}^n)^2\mathrm{d}s\leq C,
\end{aligned}$$

where C *is a positive constant independent with* h *and* Δt.

Proof. Taking $\mathbf{v}_{i,h}=\hat{\mathbf{u}}_{i,h}^{n+1}$ with $i=1,2$ in (4) and adding the ensuing equations, we have

$$\begin{aligned}
&\frac{1}{2\Delta t}\sum_{i=1}^{2}(\|\hat{\mathbf{u}}_{i,h}^{n+1}\|_0^2-\|\mathbf{u}_{i,h}^n\|_0^2+\|\hat{\mathbf{u}}_{i,h}^{n+1}-\mathbf{u}_{i,h}^n\|_0^2)+\frac{1}{2}\sum_{i=1}^{2}r_i(\|\nabla\hat{\mathbf{u}}_{i,h}^{n+1}\|_0^2-\|\nabla\mathbf{u}_{i,h}^n\|_0^2+\|\nabla\hat{\mathbf{u}}_{i,h}^{n+1}-\nabla\mathbf{u}_{i,h}^n\|_0^2)\\
&\quad+\sum_{i=1}^{2}\nu_i\|\nabla\hat{\mathbf{u}}_{i,h}^{n+1}\|_0^2+Q^{n+1}\int_I \kappa|\mathbf{u}_{1,h}^n-\mathbf{u}_{2,h}^n|(\mathbf{u}_{1,h}^n-\mathbf{u}_{2,h}^n)\hat{\mathbf{u}}_{1,h}^{n+1}\mathrm{d}s+Q^{n+1}\int_I \kappa|\mathbf{u}_{2,h}^n-\mathbf{u}_{1,h}^n|(\mathbf{u}_{2,h}^n-\mathbf{u}_{1,h}^n)\hat{\mathbf{u}}_{2,h}^{n+1}\mathrm{d}s\\
&=\sum_{i=1}^{2}(\mathbf{f}_i^{n+1},\hat{\mathbf{u}}_{i,h}^{n+1}),
\end{aligned} \tag{13}$$

where we have used the polarization identity $2a\cdot(a-b)=|a|^2+|a-b|^2-|b|^2$ and the skew-symmetric property of trilinear term. Besides, multiplying the scalar equation (5) by Q^{n+1} gains

$$\begin{aligned}&\frac{|Q^{n+1}|^2-|Q^n|^2+|Q^{n+1}-Q^n|^2}{2\Delta t}\\&=Q^{n+1}\left(\int_I\kappa|\mathbf{u}_{1,h}^n-\mathbf{u}_{2,h}^n|(\mathbf{u}_{1,h}^n-\mathbf{u}_{2,h}^n)\hat{\mathbf{u}}_{1,h}^{n+1}\mathrm{d}s+\int_I\kappa|\mathbf{u}_{2,h}^n-\mathbf{u}_{1,h}^n|(\mathbf{u}_{2,h}^n-\mathbf{u}_{1,h}^n)\hat{\mathbf{u}}_{2,h}^{n+1}\mathrm{d}s\right)\\&\quad+(Q^{n+1})^2\left(\int_I\kappa|\mathbf{u}_{1,h}^n-\mathbf{u}_{2,h}^n|(\mathbf{u}_{2,h}^n-\mathbf{u}_{1,h}^n)\mathbf{u}_{1,h}^n\mathrm{d}s+\int_I\kappa|\mathbf{u}_{2,h}^n-\mathbf{u}_{1,h}^n|(\mathbf{u}_{1,h}^n-\mathbf{u}_{2,h}^n)\mathbf{u}_{2,h}^n\mathrm{d}s\right).\end{aligned}\tag{14}$$

Then, combining (13) and (14) and multiplying the ensuing equation by $2\Delta t$ lead to

$$\begin{aligned}&\sum_{i=1}^2(\|\hat{\mathbf{u}}_{i,h}^{n+1}\|_0^2-\|\mathbf{u}_{i,h}^n\|_0^2+\|\hat{\mathbf{u}}_{i,h}^{n+1}-\mathbf{u}_{i,h}^n\|_0^2)+\sum_{i=1}^2r_i\Delta t\left(\|\nabla\hat{\mathbf{u}}_{i,h}^{n+1}\|_0^2-\|\nabla\mathbf{u}_{i,h}^n\|_0^2+\|\nabla\hat{\mathbf{u}}_{i,h}^{n+1}-\nabla\mathbf{u}_{i,h}^n\|_0^2\right)\\&\quad+2\Delta t\sum_{i=1}^2\nu_i\|\nabla\hat{\mathbf{u}}_{i,h}^{n+1}\|_0^2+|Q^{n+1}|^2-|Q^n|^2+|Q^{n+1}-Q^n|^2+2(Q^{n+1})^2\Delta t\int_I\kappa|\mathbf{u}_{1,h}^n-\mathbf{u}_{2,h}^n|(\mathbf{u}_{1,h}^n-\mathbf{u}_{2,h}^n)^2\mathrm{d}s\\&=2\Delta t\sum_{i=1}^2(\mathbf{f}_i^{n+1},\hat{\mathbf{u}}_{i,h}^{n+1})\le\sum_{i=1}^2(\nu_i\Delta t\|\nabla\hat{\mathbf{u}}_{i,h}^{n+1}\|_0^2+\nu_i^{-1}\Delta t\|\mathbf{f}_i^{n+1}\|_{-1}^2).\end{aligned}\tag{15}$$

Next, setting $(\mathbf{v}_{i,h},q_{i,h})=(\mathbf{u}_{i,h}^{n+1},p_{i,h}^{n+1})$ with $i=1,2$ in (6) and adding the ensuing equation, we arrive at

$$\begin{aligned}&\frac{1}{2\Delta t}\sum_{i=1}^2(\|\mathbf{u}_{i,h}^{n+1}\|_0^2-\|\hat{\mathbf{u}}_{i,h}^{n+1}\|_0^2+\|\mathbf{u}_{i,h}^{n+1}-\hat{\mathbf{u}}_{i,h}^{n+1}\|_0^2)+\frac{1}{2}\sum_{i=1}^2(\nu_i+r_i)(\|\nabla\mathbf{u}_{i,h}^{n+1}\|_0^2-\|\nabla\hat{\mathbf{u}}_{i,h}^{n+1}\|_0^2)\\&\quad+\frac{1}{2}\sum_{i=1}^2(\nu_i+r_i)(\|\nabla\mathbf{u}_{i,h}^{n+1}-\nabla\hat{\mathbf{u}}_{i,h}^{n+1}\|_0^2)=0.\end{aligned}$$

Finally, multiplying above equation by $2\Delta t$, combining it with (15) and summing the ensuing inequality with respect to n from 0 to $N-1$, we get desired result. □

4. Numerical experiments

4.1. Stability test.

Set $\Omega_1=[0,1]\times[0,1]$ and $\Omega_2=[0,1]\times[-1,0]$. Obviously, the interface $I=(0,1)\times\{0\}$ in this experiment. Then, choose the initial values $\mathbf{u}_1^0=(g_{1,1}(0,x,y),g_{1,2}(0,x,y))^\top$ and $\mathbf{u}_2^0=(g_{2,1}(0,x,y),g_{2,2}(0,x,y))^\top$ with

$$g_{1,1}=x(1-x)(1-2y),\ \ g_{1,2}=y(1-y)(2x-1),\ \ g_{2,1}=x(1-x)(1+2y),\ \ g_{2,2}=y(1+y)(2x-1).$$

The boundary data $\mathbf{u}_i|_{\Gamma_i}=0$ and the body forces $\mathbf{f}_1=\mathbf{f}_2=0$. Take the mesh size $h=1/32$ and the final time $T=10$. Next, denote the kinetic energy $E(\mathbf{u})=\sum_{i=1}^2\int_{\Omega_i}|\mathbf{u}_{i,h}|^2\mathrm{d}\Omega_\mathrm{i}$.

Figure 1 displays the time evolution of the kinetic energy $E(\mathbf{u})$ and the auxiliary variable Q with some different time steps $\Delta t=0.5,\ 0.1,\ 0.05,\ 0.01$. We observe that all energy curves computed by the current algorithm show monotonic decay for all time steps and the value of the auxiliary variable Q tends to 1 when the time step Δt decreases.

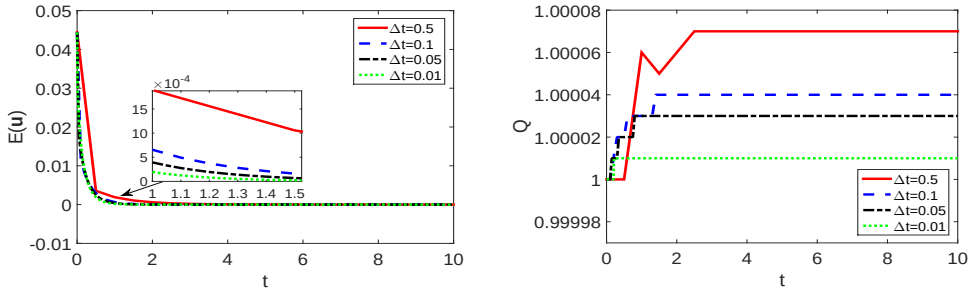

(a) (b)

Figure 1: The values of the kinetic energy (a) and scalar variable Q (b) for $\nu_1 = 0.05$, $\nu_2 = 0.1$, $\kappa = 100$ and $r_1 = r_2 = 0.15$.

4.2. Convergence rate test.

In this subsection, we present an analytical solution problem to test the convergence rate. Based on the same computational domain as the previous subsection, the analytic solution of the problem (1) is presented as follows [18]:

$$u_{1,1}(t,x,y) = -x^2\exp(-t)(x-1)^2(y-1),$$
$$u_{1,2}(t,x,y) = xy\exp(-t)(6x+y-3xy+2x^2y-4x^2-2),$$
$$u_{2,1}(t,x,y) = -x\exp(-t)(x-1)\Big(y^2x(x-1)\Big(\frac{\nu_1}{\nu_2}+1\Big) - \frac{\nu_1^{1/2}y^2\exp(t/2)}{\kappa^{1/2}} - x(x-1) + \frac{\nu_1^{1/2}\exp(t/2)}{\kappa^{1/2}} + \frac{\nu_1 xy(x-1)}{\nu_2}\Big),$$
$$u_{2,2}(t,x,y) = -\frac{y(2x-1)\exp(-t)}{3\nu_2\kappa^{1/2}}\Big(6\nu_2x^2(\kappa)^{1/2} - 6\nu_2x\kappa^{1/2} - 3\nu_1^{1/2}\nu_2\exp(t/2) - 2\nu_1x^2y^2\kappa^{1/2} - 2\nu_2x^2y^2\kappa^{1/2}$$
$$+ 3\nu_1xy\kappa^{1/2} + 2\nu_1xy^2\kappa^{1/2} - 3\nu_1x^2y\kappa^{1/2} + 2\nu_2xy^2\kappa^{1/2} + \nu_1^{1/2}\nu_2y^2\exp(t/2)\Big),$$
$$p_1(t,x,y) = p_2(t,x,y) = \exp(-t)\cos(\pi x)\sin(\pi y).$$

The chosen right-hand sides $\mathbf{f}_1 = (f_{1,1}(t,x,y), f_{1,2}(t,x,y))$ and $\mathbf{f}_2 = (f_{2,1}(t,x,y), f_{2,2}(t,x,y))$ are obliged to satisfy that $(\mathbf{u}_1, p_1)$ and $(\mathbf{u}_2, p_2)$ are the solutions of the original problem, respectively. For the sake of simplicity, we denote the errors $err(\mathbf{u}_i^N) = \|\mathbf{u}_i(t_N) - \mathbf{u}_i^N\|_0$ and

$$Err(\mathbf{u}_i) = \left(\Delta t\sum_{n=1}^{N}\|\nabla(\mathbf{u}_i(t_n) - \mathbf{u}_i^n)\|_0^2\right)^{\frac{1}{2}}, \quad Err(p_i) = \left(\Delta t\sum_{n=1}^{N}\|p_i(t_n) - p_i^n\|_0^2\right)^{\frac{1}{2}}.$$

Next, we set the value of parameters $\kappa = 100$, $r_1 = r_2 = 0.1$, $\nu_1 = 5.0E-2$ and $\nu_2 = 1.0E-1$. Four values of the mesh size $h = \Delta t = 1/4, 1/16, 1/32$ and $1/64$ are picked to verify the convergence rate. Moreover, the convergence rates of the current algorithm on the subdomains Ω_1 and Ω_2 are shown in Figure 2, which shows that the proposed algorithm works well and keeps optimal convergence rate. To further verify the spatial convergence rate for the L^2-norm of the velocity, we select a final time $T = 1.0E-2$, fix $\Delta t = T/10$, and then compute on successively refined uniform meshes. For temporal convergence, we choose the time step $\Delta t = h^2$ and vary the mesh sizes $h = 1/4, 1/8, 1/16, 1/24$ and $1/32$. Errors and convergence rates are showed in Figure 3. As expected, from this figure, we find that the current algorithm keeps the convergence rates.

4.3. Submarine mountain problem.

In this example, we test the proposed algorithm by a practical problem, called submarine mountain problem [1, 16]. Set $\Omega_1 = [0,1]\times[0,0.1]$ and $\Omega_2 = \{(x,y) : \frac{7}{40}\Big(\sin(\frac{7}{2}) - (2x-1)\sin(7x-\frac{7}{2})\Big) \le y \le 0, 0 \le x \le 1\}$.

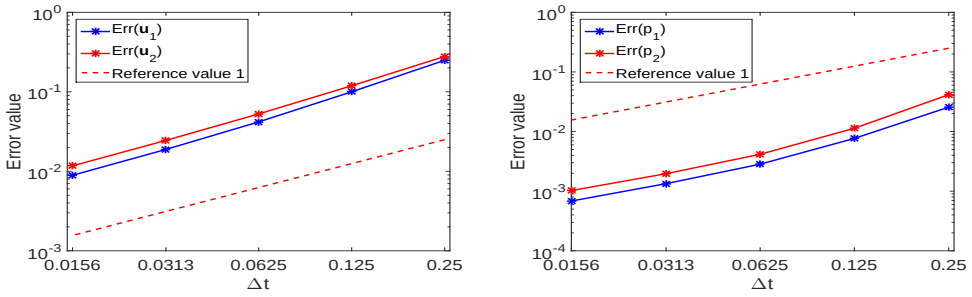

(a) (b)

Figure 2: Errors and convergence rates for the velocity field (a), pressure (b) with $T = 1$, $\Delta t = h$.

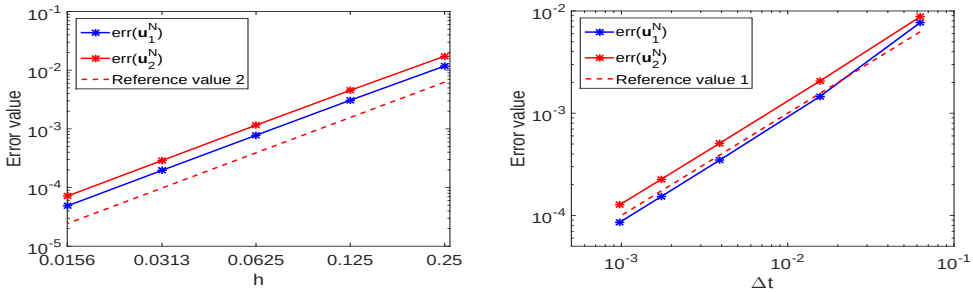

(a) (b)

Figure 3: Errors and spatial convergence rates (a), and temporal convergence rates (b) of the velocity field.

The body forces $\mathbf{f}_1$ and $\mathbf{f}_2$ are chosen to ensure that

$$
\begin{aligned}
u_{1,1}(t,x,y) &= \nu_1 \exp(-2t)x^2(1-x)^2(1+y) + \exp(-t)x(1-x)\nu_1/\sqrt{\kappa},\\
u_{1,2}(t,x,y) &= \nu_1 \exp(-2t)xy(2+y)(1-x)(2x-1) + \exp(-t)y(2x-1)\nu_1/\sqrt{\kappa},\\
u_{2,1}(t,x,y) &= \nu_1 \exp(-2t)x^2(1-x)^2(1+\nu_1/\nu_2 y),\\
u_{2,2}(t,x,y) &= \nu_1 \exp(-2t)xy(1-x)(2x-1)(2+\nu_1/\nu_2 y),\\
p_1(t,x,y) &= p_2(t,x,y) = \exp(-t)\cos(\pi x)\sin(\pi y),
\end{aligned}
$$

is the solution of problem (1). Besides, the initial values and boundary terms on Γ_i are chosen by the above exact solution. Note that if you compute the jump using the above solution, then you will realize that when $y = 0$ there exists jump. In fact, we have $u_{1,1}(t,x,0) - u_{2,1}(t,x,0) = \exp(-t)x(1-x)\nu_1/\sqrt{\kappa}$. Hence, the interface interaction will appear.

Considering the viscosity of fluid in atmosphere is smaller than that in ocean, we choose $\nu_1 = 5.0E-3$ and $\nu_2 = 5.0E-1$. Besides, we fix $\Delta t = h = 1/64$, $\kappa = 100$ and $T = 1$. Figure 4 presents numerical results of the velocity by the proposed algorithm and the geometric averaging algorithm [6]. From this figure, we see that, for the small viscosity problem, the numerical results of the current algorithm has better numerical results than that of the geometric averaging algorithm.

Acknowledgments

The authors would like to thank the editor and anonymous reviewers for their helpful comments and suggestions.

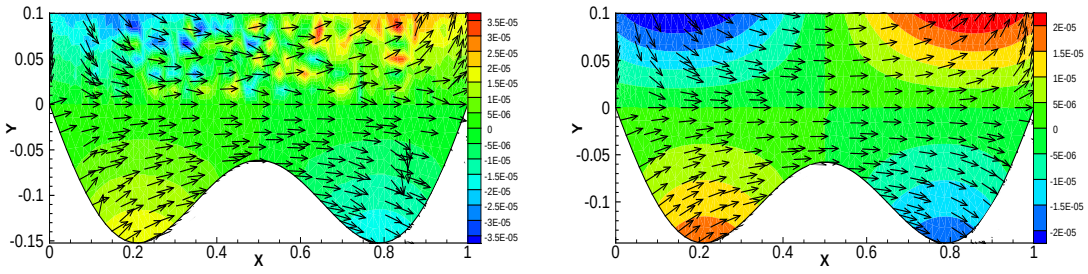

(a) (b)

Figure 4: Plots of the velocity by the geometric averaging algorithm (a) and the proposed algorithm (b) with $r_1 = r_2 = 5.0E - 1$.

References

[1] M. Aggul, A grad-div stabilized penalty projection algorithm for fluid-fluid interaction, Appl. Math. Comput. **414** (2022), 126670.
[2] M. Aggul, J. M. Connors, D. Erkmen, A. E. Labovsky, A defect-deferred correction method for fluid-fluid interaction, SIAM J. Numer. Anal. **56** (2018), 2484-2512.
[3] M. Aggul, F. G. Eroglu, S. Kaya, A. E. Labovsky, A projection based variational multiscale method for a fluid-fluid interaction problem, Comput. Methods Appl. Mech. Engrg. **365** (2020), 112957.
[4] M. Aggul, S Kaya, Defect-deferred correction method based on a subgrid artificial viscosity model for fluid-fluid interaction, Appl. Numer. Math. **160** (2021), 178-191.
[5] J. M. Connors, J. S. Howell, A fluid-fluid interaction method using decoupled subproblems and differing time steps, Numer. Meth. Part. Differ. Equs. **28** (2012), 1283-1308.
[6] J. M. Connors, J. S. Howell, W. J. Layton, Decoupled time stepping methods for fluid-fluid interaction, SIAM J. Numer. Anal. **50** (2012), 1297-1319.
[7] P. Z. Huang, T. Zhang, Z. Y. Si, A stabilized Oseen iterative finite element method for stationary conduction-convection equations, Math. Meth. Appl. Sci. **35** (2012), 103-118.
[8] P. Z. Huang, W. Q. Li, Z. Y. Si, Several iterative schemes for the stationary natural convection equations at different Rayleigh numbers, Numer. Meth. Part. Differ. Equs. **31** (2015),761-776.
[9] W. Li, P. Z. Huang, A two-step decoupled finite element algorithm for a nonlinear fluid-fluid interaction problem, Univ. Politeh. Buchar. Sci. Bull. Ser. A Appl. Math. Phys. **81** (2019), 107-118.
[10] W. Li, P. Z. Huang, Y. N. He. Grad-div stabilized finite element schemes for the fluid-fluid interaction model, Commun. Comput. Phys. **30** (2021), 536-566.
[11] W. Li, P. Z. Huang, Y. N. He, Second order unconditionally stable and convergent linearized scheme for a fluid-fluid interaction model, J. Comput. Math. **41** (2023), 72-93.
[12] W. Li, P. Z. Huang, Y. N. He, An unconditionally energy stable finite element scheme for a nonlinear fluid-fluid interaction model, IMA J. Numer. Anal. (2023), doi: 10.1093/imanum/drac086.
[13] J. Li, P. Z. Huang, J. Su, Z. X. Chen, A linear, stabilized, non-spatial iterative, partitioned time stepping method for the nonlinear Navier-Stokes/Navier-Stokes interaction model, Bound. Value Probl. **2019** (2019), 115.
[14] J. Li, P. Z. Huang, C. Zhang, G. H. Guo, A linear, decoupled fractional time-stepping method for the nonlinear fluid-fluid interaction, Numer. Methods Part. Differ. Equs. **35** (2019), 1873-1889.
[15] J. L. Lions, R. Temam, S. Wang, Mathematical theory for the coupled atmosphere-ocean models (CAO III), J. Math. Pures. Appl. **74** (1995), 105-163.
[16] L. Z. Qian, J. R. Chen, X. L. Feng, Local projection stabilized and characteristic decoupled scheme for the fluid-fluid interaction problems, Numer. Meth. Part. Differ. Equ. **33** (2017), 704-723.
[17] J. Shen, J. Xu, Convergence and error analysis for the scalar auxiliary variable (SAV) schemes to gradient flows, SIAM J. Numer. Anal. **56** (2018), 2895-2912.
[18] Y. H. Zhang, Y. R. Hou, L. Shan, Stability and convergence analysis of a decoupled algorithm for a fluid-fluid interaction problem, SIAM J. Numer. Anal. **54** (2016), 2833-2867.
[19] T. Zhang, D. Pedro, J. Y. Yuan, A large time stepping viscosity-splitting finite element method for the viscoelastic flow problem, Adv. Comput. Math. **41** (2015), 149-190.